Materials Innovations

HΣXA Publishers

Nanoparticles | Research Article | http://doi.org/10.54738/MI.2022.2701

Synthesis and Characterization of N-Modified TiO_2 Nano-powders for Efficient Removal of Rhodamine B Dye under Natural Sun Irradiation

Sameera Ghafoor[1], Rabya Aslam[1]*, Abdullah Khan Durrani[1]

1 Institute of Chemical Engineering & Technology, University of the Punjab, Lahore, Pakistan

OPEN ACCESS

Received: 25 November 2021

Accepted: 10 June 2022

Published: 30 July 2022

Citation: Ghafoor S, Aslam R, Durrani AK (**2022**) Synthesis and Characterization of N-Modified TiO_2 Nano-powders for Efficient Removal of Rhodamine B Dye under Natural Sun Irradiation. *Materials Innovations 2* (7), 176-187.

***Correspondence**: (Rabya Aslam)
rabya.icet@pu.edu.pk

Published By Hexa Publishers

ISSN
Electronic: 2790-1963

In this work, Nitrogen modified TiO_2 nanoparticles were successfully synthesized via fast acid catalyzed sol-gel route with ammonia solution as a primary nitrogen precursor. The effect of amount of nitrogen was investigated by further incorporating secondary nitrogen in prepared sample with urea precursor by adopting wet impregnation approach. Pure TiO_2 nanoparticles were also synthesized for comparison. Prepared photo-catalysts were characterized by Fourier-Transform Infrared spectroscopy, X-Ray diffraction and diffuse reflectance spectroscopic analysis. XRD results confirmed the formation of anatase crystalline phase for all prepared samples. Laboratory test experiments on Rhodamine B (RhB) decomposition under artificial visible light (20W White LED) revealed the highest photocatalytic activity of catalyst doubly doped with ammonia solution and urea whereas pure TiO_2 showed poor activity under visible light illumination. The effect of operational parameters such as catalyst dose, solution pH and substrate concentration on photocatalytic efficiency was also evaluated to obtain optimal conditions. Photocatalysis of RhB under natural sunlight with doubly-doped photo-catalyst (T5N2) showed remarkable photocatalytic performance of 99.9% after 1 hour illumination.

Keywords: Solar Photocatalysis, Urea, TiO2 Nanopowders, Nitrogen Doping, Sol-gel Synthesis

INTRODUCTION

Synthetic Dyes are organic compounds extensively used in textile industry to impart vibrant colors to the commodities, however, during wet coloring stage, a significant amount of these dyes does not bind to fabric and thus released to the environment as waste posing serious environmental concern.[1] Drainage of such dye contaminated effluent without treatment into freshwater bodies, adversely affects not only the aquatic ecosystem but can also pose serious health problems to humans[2].

Owing to their stability to light as well as bacterial decay, most of the dyes stays in the environment for a long period of time not only retarding natural water purification process but hinders sunlight penetration as well which in turn reduces photosynthetic activity under water putting a serious threat on survival of aquatic life.[3] Further, their exposure to humans and other living beings is a major health concern as these dyes are known to be potential carcinogenic and mutagenic substances[4].

In view of the toxicity of these compounds, various physical separation and chemical mineralization methods have been researched to cater the problem in a best possible way.[5,6]

Semiconductor-based heterogeneous photocatalytic mineralization has gained importance since few decades as a promising technology powered by free and renewable solar energy for water detox application[7–9]. Titanium Dioxide (TiO_2) is termed as "golden" photocatalyst due to its remarkable features of chemical, biological and photo-stability, non-toxicity and low cost[10] . However, the main hindrance in the way of pure TiO_2 application under natural sunlight is its large bandgap of 3.2eV, thus only ultraviolet rays have enough energy to excite the semiconductor material to undergo Redox reactions[11] . As Solar spectrum consists of only 5-8% UV radiation while 40% of the spectrum is based on visible light[12] , efforts have been made to shift the activation of TiO_2 towards visible part of spectrum by lowering its bandgap through the addition of other elemental dopants into the crystalline structure of the material.[13,14]

Among metallic and non-metallic dopants, non-metal atoms are proved to be more feasible and effective in enhancing visible light photoactivity by narrowing the bandgap. Several studies have been made on insertion of non- metallic atoms such as Nitrogen[15] , Carbon[16] , Sulphur[17] , and Fluorine[18] whereas Nitrogen (N) is considered as low cost, promising and efficient dopant in terms of reducing bandgap and enhancing photoactivity[19] . Yang and coworkers prepared N-doped titania by employing solvothermal route with reaction system of ethylene-diamine at 120°C and showed that increasing amount of dopant caused absorption edge to be red shifted towards visible light region[20] . Peng and fellows reported hydrothermal synthesis of N-doped titania at 140°C with triethanol-amine nitrogen precursor for Methyl orange decomposition to confirm the role of nitrogen in shifting optical absorption towards visible region[21] . A.Sanchez-Martinez reported a simple co-precipitation doping route for examining the effect of nitric acid volume on catalyst optical properties for Rhodamine B decolorization[22] . A surfactant assisted sol gel route was employed by R.P Barkul et al with different mol% of urea precursor for nitrogen doping and demonstrated good efficiency of photocatalyst with high mol% of urea for cationic dye degradation[23] .

The characteristic features and photocatalytic performance of semiconductor is greatly affected by the adopted synthesis method. Sol-Gel is a relatively low cost technique offering the use of mild processing conditions of temperature and pressure yet providing benefits of controlling size of particle, morphology and other desirable features in the final product[24,25] .

The current study deals with the synthesis of nitrogen modified TiO_2 Nano-powders by adopting alcohol free fast Sol-Gel process with ammonium hydroxide as a primary nitrogen precursor. The adopted procedure follows direct hydrolysis of Titanium precursor at room temperature, facilitated by acetic acid, allowing the completion of Sol-Gel reactions within short time. Afterwards the amount of nitrogen impurity was enhanced by wet impregnation using urea precursor. For comparative study, pure TiO_2 nanoparticles were also synthesized. The activity of prepared nanoparticles was investigated by photocatalysis of model pollutant Rhodamine B dye under artificial 20W white LED lamp and natural sunlight for practical application.

EXPERIMENTAL SETUP

Materials

Titanium (IV) isopropoxide (TTIP, 97%, Sigma Aldrich), Urea crystals (H_2NCONH_2, 99%, Merck), Glacial Acetic Acid (CH_3COOH, 99.99%, Merck), Ammonium Hydroxide NH_4OH (33% solution), Sodium Hydroxide (NaOH), Hydrochloric acid (HCl), Rhodamine B dye (BDH Chemicals). All reagents were used as received without any further purification.

Photocatalyst Preparation

A simple fast Sol Gel route as reported in reference[26] has been adopted with some modifications. 40ml of TTIP was added directly into distilled water (16^oC) and the suspension was immediately stirred on magnetic stirrer. After 30min, Glacial Acetic acid was added such that the molar ratio of TTIP: Distilled H_2O: Acetic Acid was maintained as 1:172:12. The colloidal suspension was left under continuous stirring for 3hr after which Ammonium Hydroxide (33%) solution was added to raise the pH of solution to 11. Precipitates formed were washed 3 times by adding distilled water and decanting after settling of particles. Sludge produced was then dried in air oven at 100°C till dried powders were obtained. Particles were crushed in mortar and pestle and calcined at 400°C for 1h[27,28] . The sample was labeled as T5N1.

The effect of amount of nitrogen on activity of photocatalyst was also analyzed by incorporating secondary nitrogen dopant (urea) into as-prepared catalyst (T5N1) via wet impregnation route. For this, 2g of T5N1 was added in 50ml of distilled water to make homogenous colloidal suspension to which urea solution (keeping urea to TiO_2 molar ratio 1:1) was added and the mixture was agitated for 1h at room temperature. The temperature was then raised to 68°C and mixture was kept under stirring for further 30 min after which the solvent was evaporated by heating in open beaker at 100°C. Obtained paste was dried and the powders were baked at 350°C for 1h. The sample was named as T5N2.

For comparative study, pure TiO_2 nanoparticles were also synthesized via similar sol gel methodology as adopted for T5N1 sample except sodium hydroxide was used instead of ammonium hydroxide for precipitation. Obtained powders were washed several times with distilled water, oven dried and calcined at 400^{o}C for 1h.

Characterization

Fabricated nanoparticle samples pure and doped were subjected to FTIR spectroscopic analysis in order to determine the presence of various functional groups with Cary-630 spectrophotometer (Agilent technologies) using ATR (Attenuated Total Reflection) mode and frequency range of 400-4000 cm^{-1}. For crystallite size estimation and phase identification, X-Ray diffraction (XRD) analysis has been conducted with D2 Phaser X-ray powder diffractometer (Bruker, Germany) using Cu-Kα radiation (λ = 1.54184 Å) and scan rate of 0.020 deg/min. The patterns were obtained for the angle range of 10^o-80^o(2theta). Diffuse reflectance spectroscopy (DRS) was performed for determination of band gap energies by Jasco-V770 UV-Vis Spectrophotometer equipped with integrating sphere and the spectra were taken from 200-800 nm wavelength range.

Photocatalytic activity testing

Photocatalytic experiments were performed in a batch slurry reactor (Pyrex glass beaker) under artificial white lamp comprising of 20W portable LED. Schematic of the assembly is shown in Figure 1. In a typical procedure, 60mL of aqueous solution of RhB dye ($10mgL^{-1}$) was fed to photo-reactor placed on magnetic stirring plate. Temperature of the system was kept at 23 ± 2°C by placing the reactor in cold water bath. Photocatalyst powders were dispersed in dye solution and the suspension was stirred under dark conditions for 15 min to reach absorption-desorption equilibrium.

Light was illuminated from top and the distance of lamp was kept constant at 5.5cm from above the photo-reactor. 5ml of aliquots were withdrawn from suspension after every 30min and centrifuged to separate solid catalyst from solution. Decolorization of dye was then monitored by measuring absorbance of solution with Perkin Elmer (Lambda 25) UV-Vis Spectrophotometer at λ_{max} of 554nm. The concentration of dye in solution was evaluated from calibration curve. The percentage decolorization was then calculated by using the following equation (1).

$$\%\ Decolorization = 100 \times \frac{C_0 - C}{C_0} \quad (1)$$

Where, C_0 is initial concentration of dye in solution at time t=0 min and C is the concentration after specific time (t min) of reaction.

For experiments under natural sunlight, photocatalytic assembly was placed directly under the sun for the degradation assessment of Rhodamine B (10mg/L), with optimum load of photocatalyst powders. Dye solution pH was adjusted to 3 prior to testing. Experiments were carried out at the of Institute of Chemical Engineering and Technology, University of the Punjab Lahore, Pakistan from 27th June to 3rd July between 10:00 AM to 3:00 PM with sunlight intensity of ~100 to 40 klux.

RESULTS AND DISCUSSION

FTIR Spectroscopy

FTIR spectra of as-prepared nanoparticles is presented in Figure 2. A strong absorption band between the range of 500-750 cm^{-1} corresponds to the vibration mode of Ti-O bond[29] . In pure TiO_2 the small bands at 1343 cm^{-1} and 1413 cm^{-1} represents C-H bending vibration and asymmetric CH_3 deformation respectively[30,31] also, the presence of band at 1562 cm^{-1} is likely due to asymmetric stretch of surface adsorbed carboxylate group[32] . Further, the appearance of 3225 cm^{-1} and 1630 cm^{-1} bands are characteristic of stretching and bending mode of hydroxyl group –OH and adsorbed water species[28] . In N-doped samples, the vanishing of peaks at 1343cm^{-1} and 1413cm^{-1} and reduction of peak at 1562cm^{-1} demonstrates the elimination of adsorbed organic species. It is also observed that 1630cm^{-1} and 3225cm^{-1} peaks are much stronger in N-doped Nano-powders as compared to pure TiO_2 indicating more surface bound hydroxyl groups and water molecules which is fruitful in enhancing photocatalytic activity by capturing photo-generated holes (h^+) to form highly oxidative $OH^\bullet$ radicals[33] . Moreover, in T5N2 sample small peaks appearing at 3334cm^{-1} and 1449cm^{-1} are due to –N-O_x bond[34] and N-H stretch respectively[35] .

Diffuse Reflectance Spectroscopy

To analyze the effect of nitrogen doping on optical band gap values of as-synthesized Nano-powders, diffuse reflectance spectra (DRS) of both pure and doped samples were recorded and the results are shown in Figure 3(a). It can be observed in the DRS plot that in doped samples the optical absorption is extended towards longer wavelength region as compared to pure TiO_2.

For the calculation of band gap energies, Kubelka-Munk relation F(R) was used which is given as:

$$F(R) = \frac{(1-R)^2}{2R} \quad (2)$$

Here R denotes material reflectance. Tauc plot has been made between $(F(R)\cdot h\square)^n$ and h□ with n =0.5 for indirect allowed bandgap transition, the linear portion of graph was extrapolated by drawing a line that touches the X-axis where F(R)=0 showing band gap energies as in Figure 3(b). The estimated band-gap energies of as-prepared photocatalysts are summarized in Table 1. From the results, it

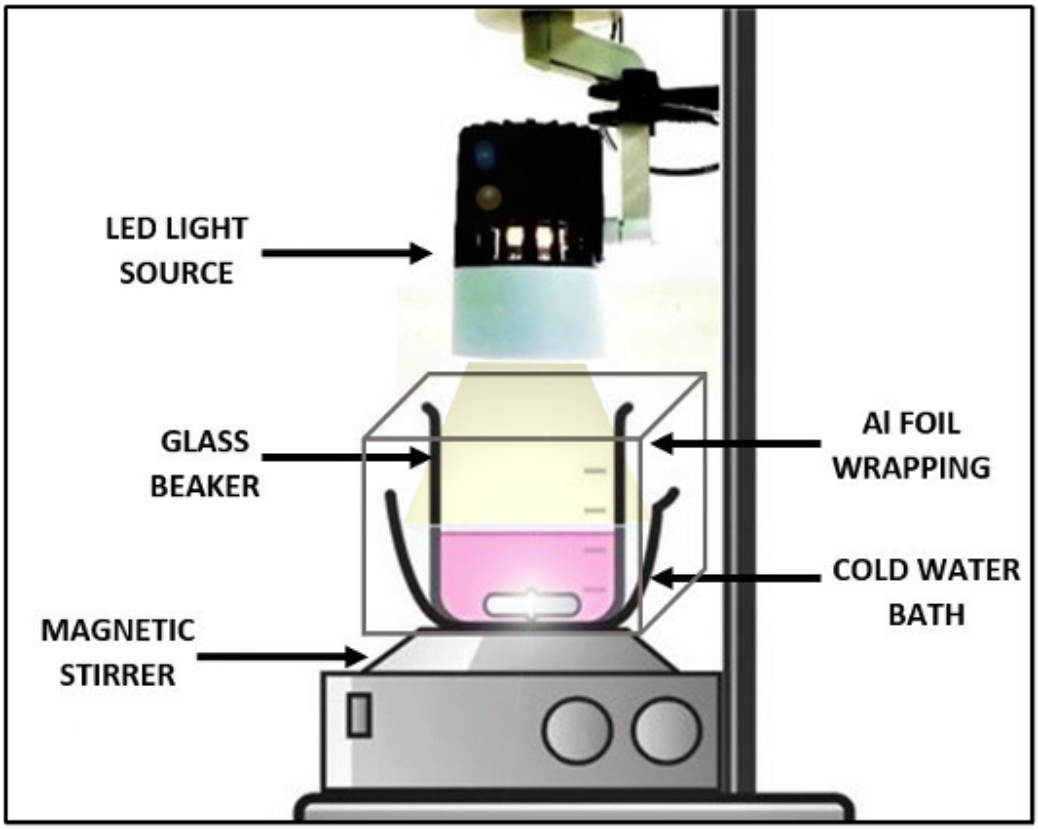

Figure 1. Photo-Reactor Setup.

is clear that the prepared sample of pure TiO_2 has a wide band gap of 3.35eV which is considerably reduced by successful incorporation of nitrogen dopant in T5N1 sample. Further lowering of band gap achieved in T5N2 sample could be attributed to increase in amount of nitrogen by urea impregnation.

It is well established that introduction of nitrogen impurity into TiO_2 creates new energy states near valence band edge which decreases the bandgap and shifts the absorption spectrum to visible wavelength region[15] . At low doping concentration, nitrogen atoms form N 2p localized states above valence band resulting in redshift of optical absorption therefore the band gap is considerably reduced to 3.08eV after primary nitrogen doping in T5N1 sample. When the amount of nitrogen is further increased in T5N2 sample, the band-gap is further reduced from 3.08 to 2.99eV which can be ascribed to the effect of overlapping of N 2p and O 2p orbitals on top of valence band thus further improving the optical absorbance of photocatalyst material in visible range[36] .

X-Ray Diffraction Analysis

The patterns obtained by diffraction analysis are depicted in Figure 4. It can be observed from the plot that all prepared samples are crystalline in nature with same phase and there is no extra peak formed in the nitrogen doped samples. Further in all samples the peaks are located at 24.6^o, 37.3^o, 47.3^o, 53.7^o, 62.2^o indexed with Miller indices as (101), (004), (200), (105), and (213) mainly associated with anatase phase according to JCPDS card file 21-1272.

The average crystallite size of prepared Nano-powders was calculated from full width at half maximum (FWHM) values corresponding to diffraction peaks by using Debye-Scherrer formula as follows:

$$D = \frac{K\lambda}{\beta cos\theta} \quad (3)$$

Where D is the crystallite size, λ is the X-Ray wavelength, β is full width at half maximum (FWHM) and θ is the Bragg's angle[23] .

The calculated average crystallite sizes for Pure TiO_2, T5N1 and T5N2 samples are reported in Table 1. It was found that all prepared samples consisted of small crystal size with no appreciable size difference between Pure and T5N1 Nano-powders. However, it was found that the crystallite size of T5N2 nanoparticles was increased which could be attributed to the influence of increasing amount of nitrogen by secondary doping.

It can be clearly observed from XRD graph that the peaks obtained for pure TiO_2 are of less intensity showing low

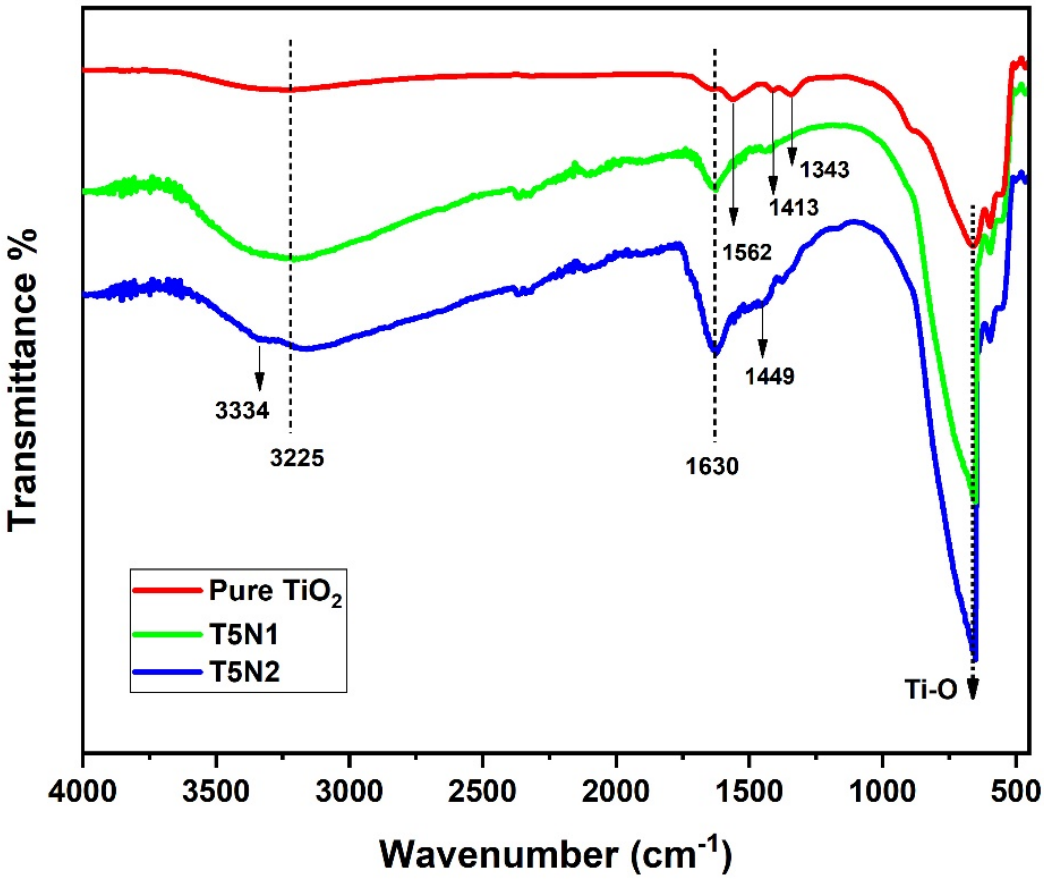

Figure 2. FTIR spectra of pure and N-doped photocatalyst powders.

anatase phase crystallinity which is greatly enhanced after nitrogen doping. This change can be attributed to the effect of strong electrostatic repulsion between Nano-powders and ammonia groups during Sol-Gel precipitation step, resulting in well dispersion of nanoparticles and enhanced anatase phase crystallinity.[37]

Furthermore, slightly broad XRD peak suggests small particle size for pure TiO_2, which upon N-Modification gets narrowed showing increase in size of the crystal as the doping level increases. This could be due to the expansion of lattice by nitrogen doping at interstitial level which led to bigger particle size as the amount of nitrogen is increased.[38]

Photocatalytic Degradation Experiments

Photocatalytic decomposition of Rhodamine B was tested over as-synthesized Pure TiO_2, T5N1 and T5N2 Nano-powders under artificial light source (pH=3). The degradation profile is depicted in Fig. 5(a). From the graph it can be observed that pure TiO_2 Nano-powders showed poor activity under visible light illumination by decomposing only 17.45% of dye under 1h irradiation. With T5N1 sample, 83.12% photocatalytic activity was achieved whereas T5N2 showed the highest degradation efficiency of 96.93% under same time duration. The enhanced activity of N-modified photocatalysts can be ascribed to the role of nitrogen in shifting the band structure of semiconductor towards visible light region and as the amount of nitrogen is increased by impregnation approach, the visible light absorption capacity of catalyst is increased further resulting in higher photocatalytic decomposition. T5N2 photocatalyst was then chosen for the rest of experimentation.

Self-fading of Rhodamine B dye under light in the absence of catalyst was also tested and it was found that no degradation of dye took place under light illumination only. The effect of photocatalyst without light illumination was also investigated by conducting experiment under dark conditions and only 4% of dye concentration was

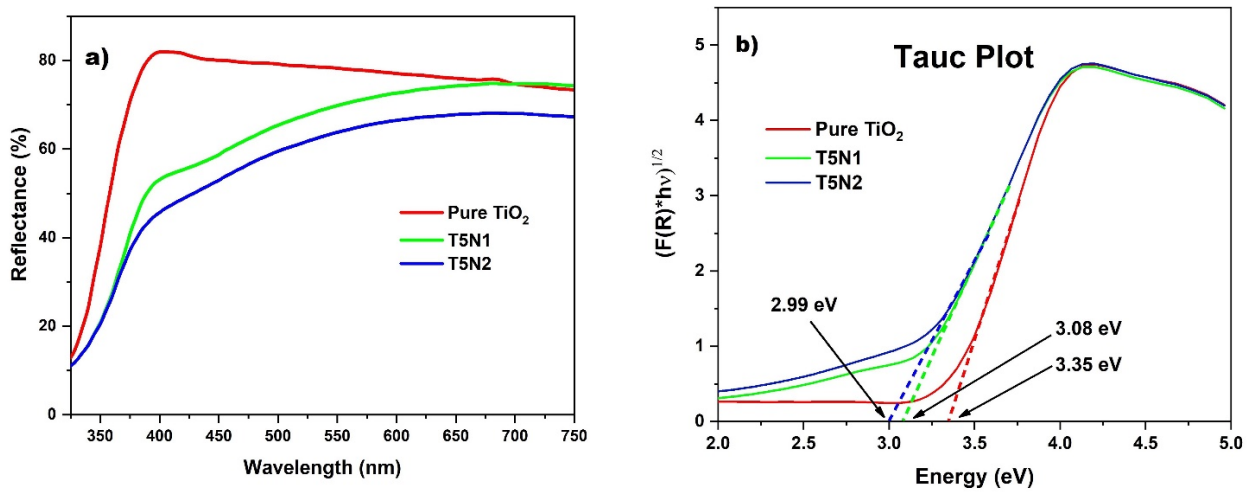

Figure 3. (a) Reflectance spectra, (b) Tauc Plot of Pure TiO_2, T5N1 and T5N2 Photocatalysts.

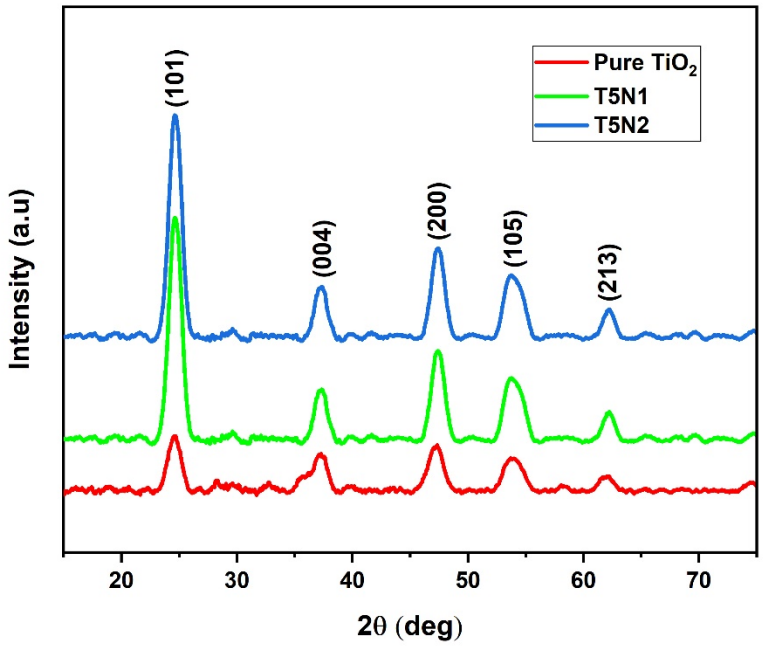

Figure 4. XRD patterns of pure and doped powders.

Table 1. Summary of Crystallite Size and Band gap energies of as-synthesized Nano-Powders

Sample	Avg. Crystallite Size (nm)	Band gap (eV)
Pure TiO_2	5.85	3.35
T5N1	5.95	3.08
T5N2	7.35	2.99

reduced after 2h which could be mainly attributed to the adsorption of dye on catalyst surface and not due to decomposition.

Kinetic Study

For most organic compounds, the photocatalytic degradation mechanism has often been described by Langmuir-Hinshelwood (L-H) kinetic model which also takes into consideration the adsorption of substrate on surface of photocatalyst as represented in Eq. (4)[39] .

$$-\frac{d(C]}{dt} = \frac{k_r K_{ads}[C]}{1 + K_{ads}[C]}$$

Where, k_r is the reaction rate constant (mgL^{-1} min^{-1}), K_{ads} is the adsorption coefficient of substrate on catalyst surface (mg^{-1} L) and [C] is the concentration of substrate (mg L^{-1}). As in case of low substrate concentration (i-e $K_{ads}[C] << 1$) the L-H equation takes the pseudo-first order kinetic form[40] (Eq.5) which is further simplified by integration as depicted in Eq. (6):

$$-\frac{d(C]}{dt} = k_{app} \times [C] \quad (5)$$

$$ln\frac{[C_0]}{(C]} = k_{app} \times t \quad (6)$$

Here $k_{app}=k_r K_{ads}$ which is the apparent first order rate constant. In order to determine the kinetics of Rhodamine B photocatalytic degradation, the equation was plotted for all prepared photocatalysts as shown in Fig. 5(b). The resulting straight lines confirmed that the dye degradation obeyed pseudo-first order kinetics. The values of apparent rate constant k_{app} evaluated from slopes of plot were $0.0033min^{-1}$, $0.0310min^{-1,}$ and $0.0714min^{-1}$ for pure TiO_2, T5N1 and T5N2 respectively. Table 2 summarizes the apparent rate constants, corresponding R^2 values and degradation percentages for respective photocatalyst powders.

Effect of Solution pH

Solution pH has a great influence on photocatalytic efficiency as changing pH affects the stability, surface charge chemistry and the redox potential of free radicals which are formed over photocatalyst surface. In order to study the effect of pH on degradation efficiency, photocatalytic tests were performed with varying initial solution pH (acidic pH 3, neutral pH 7 and basic pH 10) by keeping other parameters constant under 2 hour irradiation time. The results are plotted in Figure 5(c). At neutral pH conditions, 84.17% decomposition of dye was achieved whereas the rate of photocatalytic reaction was significantly enhanced when initial pH of solution was lowered (pH=3) resulting in 99.83% Photo-degradation. It was observed that under acidic conditions stable colloidal suspension was obtained offering high surface area for photocatalytic activity, also the lattice bound oxygen has a tendency to trap holes in presence of protons to form surface bound hydroxyl radicals resulting in enhanced photocatalytic efficiency under acidic environment[41] . When pH was increased to 10 the stability and dispersion of nanoparticles was adversely affected and agglomeration was favored which resulted in lower activity of only 52% under alkaline conditions.

Effect of Photocatalyst Dose

To study the effect of photocatalyst load on photo-degradation efficiency, experiments were performed with catalyst dose of 0.03 to 0.12g at pH=3 and room temperature conditions. It was found that as the amount of photocatalyst was increased higher degradation rates were obtained till catalyst dosage of 0.09g, this is mainly due to increase in number of active sites available for photo-absorption thus enhancing photocatalytic activity. Further increase of catalyst dose to 0.12g resulted in decreased photocatalytic efficiency which could be the effect of hindrance to light penetration in the bulk of solution due to increased turbidity of the solution with high photocatalyst dose. The obtained optimum quantity of photocatalyst was 0.09g or 1.5g/L. The results are depicted in Figure 6(a).

Effect of initial Dye Concentration

The effect of initial Rhodamine B dye concentration on photocatalytic performance was evaluated within the concentration range of 5-20mg/L and the results are illustrated in Figure 6(b). The degradation performance was found to be reduced with increase in initial dye concentration which could be attributed to the consequence of blockage of light falling on photocatalyst surface due to excessive dye molecules in solution which in turn lessens the amount of photons reaching the photocatalyst surface. This eventually limits the production of hydroxyl radicals and superoxide anions leading to decreased photocatalytic performance.

Photocatalytic Activity under Natural Sunlight Illumination

Rhodamine B (10mg/L) decomposition was tested with pure TiO_2 and T5N2 photocatalyst for 1 hour sunlight irradiation under optimum conditions of catalyst load and the solution pH was adjusted to 3 with HCl. The suspension of photocatalyst and dye solution was stirred in dark for 15 min after which the assembly was placed under direct sunlight for photocatalytic testing. Results shown in Figure 6(c) illustrate remarkable activity of T5N2 photocatalyst as compared to pure TiO_2 Nano-Powders. It was found that only 19% of dye degradation was achieved with pure TiO_2 nanopowders, however, with T5N2 photocatalyst 99.9% dye decolorization took place under similar conditions. Comparison of photocatalytic activity under artificial light source and natural sunlight with T5N2 sample revealed 3% increase in degradation performance under natural sunlight, whereas in case

Table 2. Summary of Kinetic parameters and corresponding degradation% for As-prepared Photocatalyst Powders

Photocatalyst	K_{app}(min^{-1})	Coefficient R ^{2}	Degradation (%) (Time=1h)
Pure TiO_2	0.0033	0.9959	17.45
T5N1	0.0310	0.9963	83.12
T5N2	0.0714	0.9883	96.93

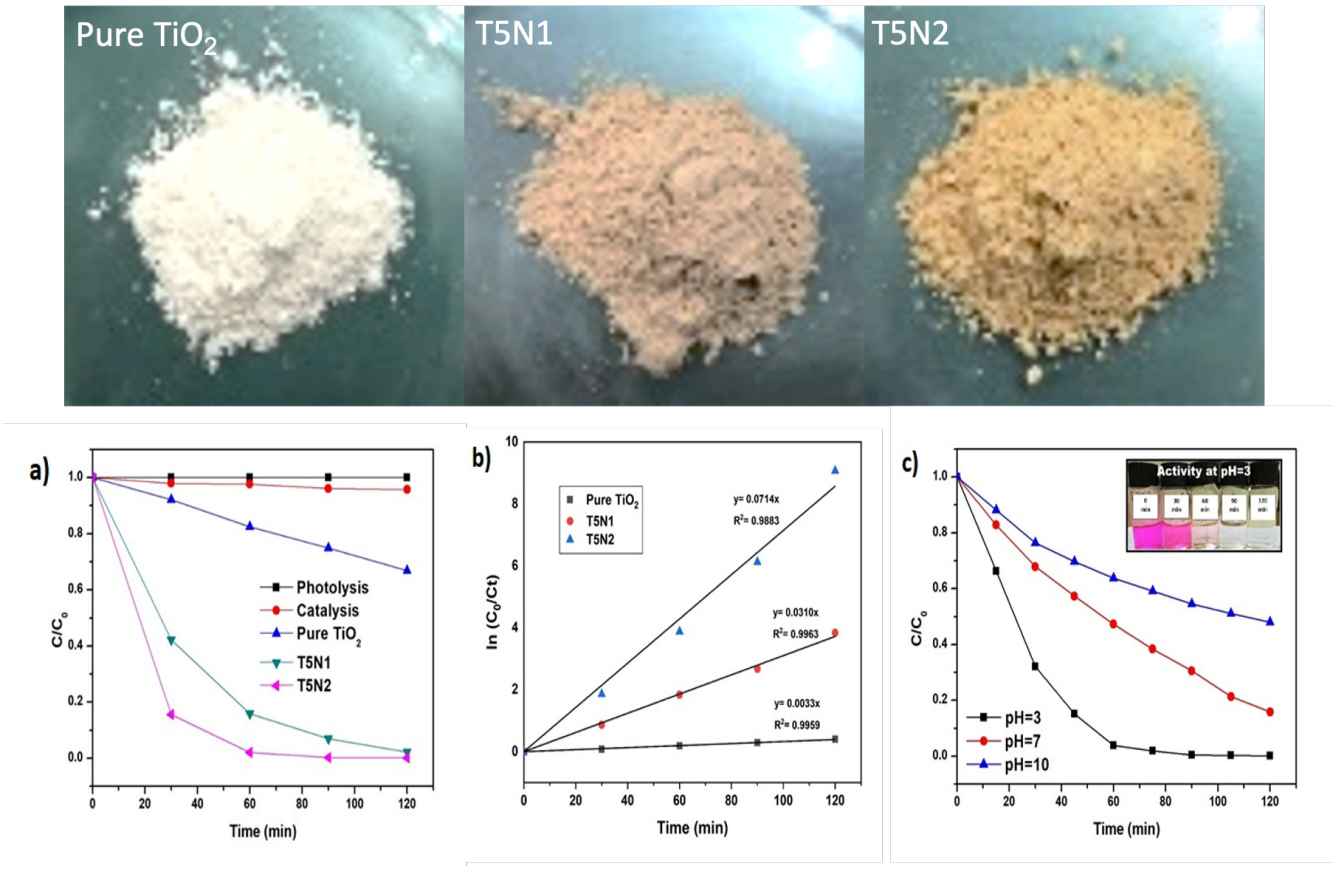

Figure 5. (a) Degradation profile of Rhodamine B dye over pure TiO_2, T5N1 and T5N2 catalysts (b) Plot of ln(C0/Ct) vs time for RhB degradation over pure and N-doped TiO_2 (c) Effect of pH on photo-degradation of Rhodamine B over T5N2 Nano-powders. Top panel shows the appearance of TiO_2, T5N1, and T5N2 samples.

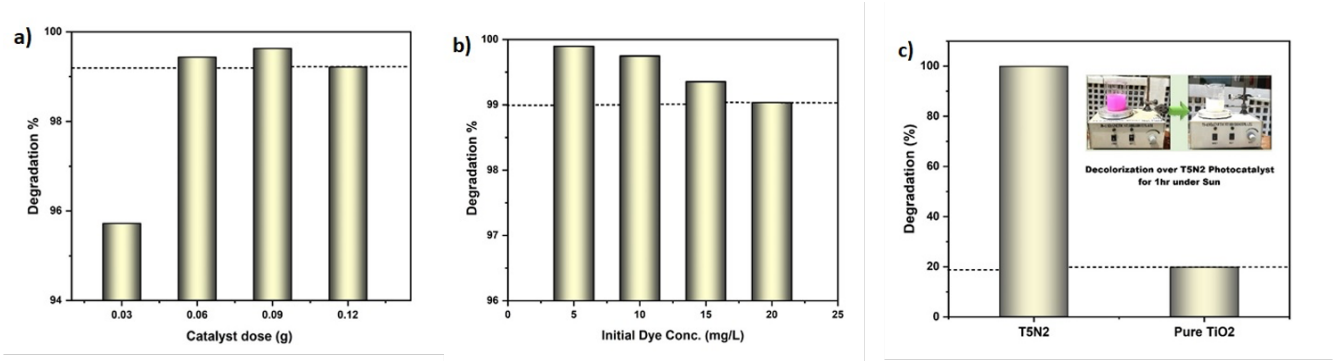

Figure 6. (a) Effect of catalyst dosage on % degradation of Rhodamine B (b) Effect of initial dye concentration on degradation efficiency of Rhodamine B (c) Comparative illustration of RhB dye degradation under natural sunlight with pure TiO_2 and T5N2 nanoparticles

of Pure TiO_2 Nano-Powders, the degradation was enhanced by 8% under Sun. Thus slightly higher activity for both photocatalysts was obtained under natural sunlight irradiation as compared to artificial lamp.

It is well known that photocatalytic activity is not only dependent on photocatalyst powder characteristics but also on the intensity and wavelength spectrum of incident light source. As the intensity of desired wavelength radiations falling on photocatalyst is increased, more electron-hole pairs are formed on photocatalyst surface leading to high rate of photocatalytic reactions[]. In our study, we have utilized LED White light which is free of UV radiations, requires less electrical energy input (20 Watts) while giving good light intensity output to check the photo-catalyst activity under only visible light radiations.

For experiments under natural sunlight, peak summer midday time was selected at which maximum intensity of sunlight is available therefore, higher photocatalytic activity is achieved due to high intensity of incident light photons as compared to indoor experiments with artificial lamp. Also, sunlight spectrum contains small portion of UV radiations which can excite the photocatalyst powders as they possess higher energy than the bandgap of prepared samples[42] .Therefore, it is suggested that the higher activity of photocatalysts under sun is the consequence of high intensity visible light rays along with the presence of UV radiations.

Proposed Degradation Mechanism

Photocatalysis of organic pollutants is a highly complex process involving various reduction/oxidation reactions on Photocatalyst surface. The degradation mechansim starts when the light of appropriate wavelength falls on photocatalyst surface, making the electrons (e^-) in valence band (VB) to get excited and jump to the conduction band (CB) leaving behind holes (h^+) in valence band[43] . The dissolved oxygen present in solution readily captures the CB electrons to form superoxide anion which undergoes further reduction to produce hydrogen peroxide in two steps, first the superoxide anion in presence of protons form hydroperoxyl radical ($HOO^{\cdot}$) which upon reduction give hydrogen peroxide as represented in Eq (7-9).

$$O_2 + e^-_{CB} \rightarrow O_2^{-\cdot} \quad (7)$$

$$O_2^{-\cdot} + H^+ \rightarrow HOO\cdot \quad (8)$$

$$HOO\cdot + e^-_{CB} + H^+ + \rightarrow H_2O_2 \quad (9)$$

Hydroxyl radicals are then formed by dissociation of H_2O_2 and/or by the attack of highly reactive valence band holes (h^+) on the adsorbed water/OH^- (Eq. 10-12)[44] .

$$H_2O_2 + e^-_{CB} \rightarrow OH^{\cdot} + OH^- \quad (10)$$

$$H_2O_2 + O_2^{-\cdot} \rightarrow OH^{\cdot} + OH^- + O_2 \quad (11)$$

$$OH^-/H_2O + h^+_{vB} \rightarrow OH^{\cdot} \quad (12)$$

$$O_s^{2-} + H^+ + h^+_{vB} \rightarrow OH_s^{\cdot} \quad (13)$$

Furthermore, under acidic environment lattice bound oxygen trap holes to generate surface bound hydroxyl radicals[45] as in Eq-13.

The attack of these generated hydroxyl radicals on RhB molecules along with direct oxidation of RhB dye on photocatalyst surface by VB holes (h^+) eventually degrade dye pollutant into mineralization products such as carbon dioxide, water and inorganic nitrogen species ($NH_4^+$and NO_3^-).[46,47]

Apart from photocatalytic degradation pathway, photo-sensitized decolorization of Rhodamine B dye also takes place to some extent on photocatalyst surface (Eq-14-15). Rhodamine B is a sensitizer dye which itself gets excited on exposure to visible light and injects an electron to the conduction band of semiconductor which is captured by dissolve oxygen resulting in superoxide anion ($O_2^{\cdot -}$) formation. Hydroxyl radicals are then generated by the same scheme as described earlier in Eq (8-11). These active radical species subsequently reacts with RhB dye yielding degradation products.[48,49]

$$RhB + h\nu \rightarrow RhB^* \rightarrow RhB^{\cdot +} + e^-_{CB} \quad (14)$$

$$RhB/RhB^{\cdot +} + O_2^{-\cdot} + OH^{\cdot} \rightarrow Degradation\ \ Products \quad (15)$$

In the present study, slight photoactivity obtained under artificial visible light with pure TiO_2 could be attributed to the photosensitization effect since pure TiO_2 is a wide bandgap material which cannot be activated with visible light wavelengths to undergo photocatalytic degradation with electron(e^-) hole (h^+) pair formation on photocatalyst surface.

Also, it is noted that the activity of the photocatalyst was increased 4.76 times after primary nitrogen doping (T5N1) and 5.55 times after secondary doping (T5N2) which is mainly attributed to the enhanced photoabsoprtion capacity of semiconductor in visible light range by nitrogen insertion as confirmed by DRS analysis. The intraband states are created near the valence band edge with nitrogen incorporation[50] which decreases the bandgap of photocatalyst and favors the e^- transfer from VB to CB on visible light exposure. Thus Rhodamine B dye is effectively degraded by sequence of reactions under visible light active N-TiO_2 based photocatalytic system. Scheme of degradation mechansim on photocatalyst surface is represented in Figure 7.

CONCLUSIONS

Anatase phase N-modified TiO_2 nanoparticles were successfully synthesized by adopting fast acetic acid assisted Sol-Gel method with ammonia solution as primary nitrogen precursor

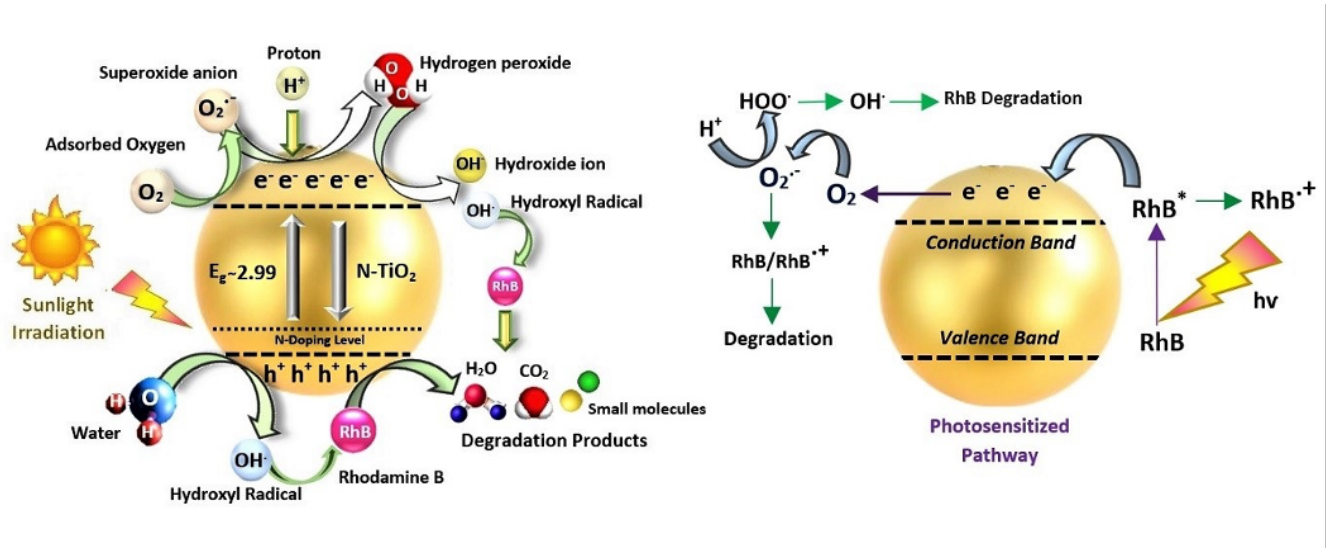

Figure 7. Proposed Degradation Mechanism of RhB over Photocatalyst Surface

(T5N1 sample). The amount of nitrogen was increased by wet-impregnation route with urea as secondary nitrogen dopant (T5N2 sample). Significant bandgap reduction with nitrogen insertion in Nano-powders was confirmed by diffuse reflectance spectroscopy. T5N2 photo-catalyst showed highest photocatalytic activity which is attributed to the effect of nitrogen impurity on lowering band gap energy of semiconductor material making the catalyst active under visible light region. Under 20W Artificial White LED with T5N2 Nano-powders, degradation of Rhodamine B was 96.93% after 1 hour whereas experiments under natural sunlight showed higher photocatalytic efficiency as compared to artificial light with 99.9% decomposition of dye within same time duration. The enhanced photocatalytic performance under free and renewable sunlight is expected to be the effect of small portion of UV radiations and high intensity of visible light photons making the process more efficient and economical. Therefore, it can be concluded that the adopted semiconductor based technology for environmental remediation is efficient and effective enough to be further investigated and practiced on real time wastewater system.

ACKNOWLEDGMENTS

The authors wish to thank Dr. Ali Rauf (LUMS, Pakistan) and Owais Sattar (BUITEMS, Quetta, Pakistan) for their help in characterization of photocatalysts. The authors declare that they have no known competing financial interests or personal relationships that could have appeared to influence the work reported in this paper.

References

1) Padhi, B. Pollution due to synthetic dyes toxicity & carcinogenicity studies and remediation. *International Journal of Environmental Sciences* **2012**, *3* (3), 940–940.
2) Lellis, B.; Fávaro-Polonio, C. Z.; Pamphile, J. A.; Polonio, J. C. Effects of textile dyes on health and the environment and bioremediation potential of living organisms. *Biotechnology Research and Innovation* **2019**, *3* (2), 275–290.
3) Pereira, L.; Alves, M. In *Dyes-environmental impact and remediation, in Environmental protection strategies for sustainable development*; and others„ Ed.; Springer, 2012; pp 111–162.
4) Chequer, F. M. D.; Dorta, D. J.; De Oliveira, D. P. Azo dyes and their metabolites: does the discharge of the azo dye into water bodies represent human and ecological risks? Advances in treating textile effluent . 2011.
5) Ortolano, L.; Sanchez-Triana, E.; Afzal, J.; Ali, C. L.; Rebellón, S. A. Cleaner production in Pakistan's leather and textile sectors. *Journal of Cleaner Production* **2014**, *68*, 121–129.
6) Holkar, C. R.; Jadhav, A. J.; Pinjari, D. V.; Mahamuni, N. M.; Pandit, A. B. A critical review on textile wastewater treatments: Possible approaches. *Journal of Environmental Management* **2016**, *182*, 351–366.
7) Herrmann, J. M. Heterogeneous photocatalysis: state of the art and present applications In honor of Pr. *Topics in catalysis* **1912**, *34* (1-4), 49–65.
8) Ye, G.; Yu, Z.; Li, Y.; Li, L.; Song, L.; Gu, L.; Cao, X. Efficient treatment of brine wastewater through a flow-through technology integrating desalination and photocatalysis. *Water Research* **2019**, *157*, 134–144.
9) Yang, Y.; Li, X.; Zhou, C.; Xiong, W.; Zeng, G.; Huang, D.; Zhang, C.; Wang, W.; Song, B.; Tang, X.; Li, X.; Guo, H. Recent advances in application of graphitic carbon nitride-based catalysts for degrading organic contaminants in water through advanced oxidation processes beyond photocatalysis: A critical review. *Water Research* **2020**, *184*, 116200–116200.
10) Guo, Q.; Zhou, C.; Ma, Z.; Yang, X. Fundamentals of TiO2 Photocatalysis: Concepts, Mechanisms, and Challenges. *Advanced Materials* **2019**, *31* (50), 1901997–1901997.
11) Nolan, N. T.; Synnott, D. W.; Seery, M. K.; Hinder, S. J.; Wassenhoven, A. V.; Pillai, S. C. Effect of N-doping on the photocatalytic activity of sol–gel TiO2. *Journal of Hazardous Materials* **2012**, *211-212*, 88–94.
12) Shahbazkhany, S.; Salehi, M.; Mousavi-kamazani, M. Facile synthesis, characterization, and decolorization activity of Mn 2+ and Al 3+ co-doped hexagonal-like ZnO nanostructures as photocatalysts. *Applied Organometallic Chemistry* **2020**, *34* (3), 5346–5346.

13) Zhang, Y.; Wang, L.; Liu, D.; Gao, Y.; Song, C.; Shi, Y.; Qu, D.; Shi, J. Morphology effect of honeycomb-like inverse opal for efficient photocatalytic water disinfection and photodegradation of organic pollutant. *Molecular Catalysis* **2018**, *444*, 42–52.
14) Burda, C.; Lou, Y.; Chen, X.; Samia, A. C. S.; Stout, J.; Gole, J. L. Enhanced Nitrogen Doping in TiO2 Nanoparticles. *Nano Letters* **2003**, *3* (8), 1049–1051.
15) Ansari, S. A.; Khan, M. M.; Ansari, M. O.; Cho, M. H. Nitrogen-doped titanium dioxide (N-doped TiO2) for visible light photocatalysis. *New Journal of Chemistry* **2016**, *40* (4), 3000–3009.
16) Yang, Y.; Ni, D.; Yao, Y.; Zhong, Y.; Ma, Y.; Yao, J. High photocatalytic activity of carbon doped TiO2 prepared by fast combustion of organic capping ligands. *RSC Advances* **2015**, *5* (113), 93635–93643.
17) Mcmanamon, C.; O'connell, J.; Delaney, P.; Rasappa, S.; Holmes, J. D.; Morris, M. A. A facile route to synthesis of S-doped TiO2 nanoparticles for photocatalytic activity. *Journal of Molecular Catalysis A: Chemical* **2015**, *406*, 51–57.
18) Yu, W.; Liu, X.; Pan, L.; Li, J.; Liu, J.; Zhang, J.; Li, P.; Chen, C.; Sun, Z. Enhanced visible light photocatalytic degradation of methylene blue by F-doped TiO2. *Applied Surface Science* **2014**, *319*, 107–112.
19) Cheng, X.; Yu, X.; Xing, Z.; Wan, J. Enhanced Photocatalytic Activity of Nitrogen Doped TiO2 Anatase Nano-Particle under Simulated Sunlight Irradiation. *Energy Procedia* **2012**, *16*, 598–605.
20) Yang, G.; Jiang, Z.; Shi, H.; Xiao, T.; Yan, Z. Preparation of highly visible-light active N-doped TiO2 photocatalyst. *Journal of Materials Chemistry* **2010**, *20* (25), 5301–5301.
21) Peng, F.; Cai, L.; Huang, L.; Yu, H.; Wang, H. Preparation of nitrogen-doped titanium dioxide with visible-light photocatalytic activity using a facile hydrothermal method. *Journal of Physics and Chemistry of Solids* **2008**, *69* (7), 1657–1664.
22) Sanchez-Martinez, A.; Ceballos-Sanchez, O.; Koop-Santa, C.; López-Mena, E. R.; Orozco-Guareño, E.; García-Guaderrama, M. N-doped TiO2 nanoparticles obtained by a facile coprecipitation method at low temperature. *Ceramics International* **2018**, *44* (5), 5273–5283.
23) Barkul, R. P.; Koli, V. B.; Shewale, V. B.; Patil, M. K.; Delekar, S. D. Visible active nanocrystalline N-doped anatase TiO2 particles for photocatalytic mineralization studies. *Materials Chemistry and Physics* **2016**, *173*, 42–51.
24) Ullattil, S. G.; Periyat, P. Sol-Gel Synthesis of Titanium Dioxide. *Advances in Sol-Gel Derived Materials and Technologies* **2017**, 271–283.
25) Tseng, T. K.; Lin, Y. S.; Chen, Y. J.; Chu, H. A Review of Photocatalysts Prepared by Sol-Gel Method for VOCs Removal. *International Journal of Molecular Sciences* **2010**, *11* (6), 2336–2361.
26) Leyva-Porras, C.; Toxqui-Teran, A.; Vega-Becerra, O.; Miki-Yoshida, M.; Rojas-Villalobos, M.; García-Guaderrama, M.; Aguilar-Martínez, J. A. Low-temperature synthesis and characterization of anatase TiO2 nanoparticles by an acid assisted sol–gel method. *Journal of Alloys and Compounds* **2015**, *647*, 627–636.
27) Kisch, H.; Sakthivel, S.; Janczarek, M.; Mitoraj, D. A Low-Band Gap, Nitrogen-Modified Titania Visible-Light Photocatalyst. *The Journal of Physical Chemistry C* **2007**, *111* (30), 11445–11449.
28) Tryba, B.; Wozniak, M.; Zolnierkiewicz, G.; Guskos, N.; Morawski, A.; Colbeau-Justin, C.; Wrobel, R.; Nitta, A.; Ohtani, B. Influence of an Electronic Structure of N-TiO2 on Its Photocatalytic Activity towards Decomposition of Acetaldehyde under UV and Fluorescent Lamps Irradiation. *Catalysts* **2018**, *8* (2), 85–85.
29) Beranek, R.; Kisch, H. Tuning the optical and photoelectrochemical properties of surface-modified TiO2. Photochemical & photobiological sciences. *Photochemical & photobiological sciences* **2008**, *7*, 40–48, DOI: 10.1039/b711658f, available at https://doi.org/10.1039/b711658f.
30) Deshpande, S. B.; Potdar, H. S.; Khollam, Y. B.; Patil, K. R.; Pasricha, R.; Jacob, N. E. Room temperature synthesis of mesoporous aggregates of anatase TiO2 nanoparticles. *Materials Chemistry and Physics* **2006**, *97* (2-3), 207–212.
31) Colomer, M. Straightforward synthesis of Ti-doped YSZ gels by chemical modification of the precursors alkoxides. *Journal of Sol-Gel Science and Technology* **2013**, *67* (1), 135–144.
32) Coates, J. Interpretation of infrared spectra, a practical approach. . Encyclopedia of analytical chemistry: applications, theory and instrumentation. 2006.
33) Cheng, X.; Yu, X.; Xing, Z.; Yang, L. Synthesis and characterization of N-doped TiO2 and its enhanced visible-light photocatalytic activity. *Arabian Journal of Chemistry* **2016**, *9*, S1706–S1711.
34) Huo, Y.; Jin, Y.; Zhu, J.; Li, H. Highly active TiO2−x−yNxFy visible photocatalyst prepared under supercritical conditions in NH4F/EtOH fluid. *Applied Catalysis B: Environmental* **2009**, *89* (3-4), 543–550.
35) Azami, M. S.; Nawawi, W. I.; Jawad, A. H.; Ishak, M. A. M.; Ismail, K. N-doped TiO2 Synthesised via Microwave Induced Photocatalytic on RR4 dye Removal under LED Light Irradiation. *Sains Malaysiana* **2017**, *46* (8), 1309–1316.
36) Yang, K.; Dai, Y.; Huang, B. Study of the Nitrogen Concentration Influence on N-Doped TiO2 Anatase from First-Principles Calculations. *The Journal of Physical Chemistry C* **2007**, *111* (32), 12086–12090.
37) Cheng, X.; Yu, X.; Xing, Z. Enhanced photoelectric property and visible activity of nitrogen doped TiO2 synthesized from different nitrogen dopants. *Applied Surface Science* **2013**, *268*, 204–208.
38) Ntozakhe, L.; Taziwa, R. T.; Mungondori, H. H. Influence of nitrogen doping on TiO2 nanoparticles synthesized by pneumatic spray pyrolysis method. *Materials Research Express* **2019**, *6* (8), 0850a9–0850a9.
39) Talat-Mehrabad, J.; Khosravi, M.; Modirshahla, N.; Behnajady, M. A. Synthesis, characterization, and photocatalytic activity of co-doped Ag–, Mg–TiO2P25 by photodeposition and impregnation methods. *Desalination and Water Treatment* **2016**, *57* (22), 10451–10461.
40) Isari, A. A.; Payan, A.; Fattahi, M.; Jorfi, S.; Kakavandi, B. Photocatalytic degradation of rhodamine B and real textile wastewater using Fe-doped TiO2 anchored on reduced graphene oxide (Fe-TiO2/rGO): Characterization and feasibility, mechanism and pathway studies. *Applied Surface Science* **2018**, *462*, 549–564.
41) Salvador, P. On the Nature of Photogenerated Radical Species Active in the Oxidative Degradation of Dissolved Pollutants with TiO2 Aqueous Suspensions: A Revision in the Light of the Electronic Structure of Adsorbed Water. *The Journal of Physical Chemistry C* **2007**, *111* (45), 17038–17043.
42) Reza, K. M.; Kurny, A.; Gulshan, F. 2017.
43) Etacheri, V.; Valentin, C. D.; Schneider, J.; Bahnemann, D.; Pillai, S. C. Visible-light activation of TiO2 photocatalysts: Advances in theory and experiments. *Journal of Photochemistry and Photobiology C: Photochemistry Reviews* **2015**, *25*, 1–29.
44) Ajmal, A.; Majeed, I.; Malik, R. N.; Idriss, H.; Nadeem, M. A. Principles and mechanisms of photocatalytic dye degradation on TiO2 based photocatalysts: a comparative overview. *RSC Adv.* **2014**, *4* (70), 37003–37026.
45) Schneider, J.; Matsuoka, M.; Takeuchi, M.; Zhang, J.; Horiuchi, Y.; Anpo, M.; Bahnemann, D. W. Understanding TiO2 Photocatalysis: Mechanisms and Materials. *Chemical Reviews* **2014**, *114* (19), 9919–9986.
46) Natarajan, T. S.; Thomas, M.; Natarajan, K. S.; Bajaj, H. C.; Tayade, R. J. Study on UV-LED/TiO2 process for degradation of Rhodamine B dye. *Chemical Engineering Journal* **2011**, *169* (1-3), 126–134.
47) Lee, S. Y.; Kang, D.; Jeong, S.; Do, H. T.; Kim, J. H. Photocatalytic Degradation of Rhodamine B Dye by TiO2 and Gold Nanoparticles Supported on a Floating Porous Polydimethylsiloxane Sponge under Ultraviolet and Visible Light Irradiation. *ACS Omega* **2020**, *5* (8), 4233–4241.
48) Wu, T.; Liu, G.; Zhao, J.; Hidaka, H.; Serpone, N. Photoassisted Degradation of Dye Pollutants. V. Self-Photosensitized Oxidative Transformation of Rhodamine B under Visible Light Irradiation in Aqueous

TiO₂ Dispersions. *The Journal of Physical Chemistry B* **1998**, *102* (30), 5845–5851.

49) Koh, P. W.; Hatta, M. H. M.; Ong, S. T.; Yuliati, L.; Lee, S. L. Photocatalytic degradation of photosensitizing and non-photosensitizing dyes over chromium doped titania photocatalysts under visible light. *Journal of Photochemistry and Photobiology A: Chemistry* **2017**, *332*, 215–223.

50) Zeng, L.; Song, W.; Li, M.; Jie, X.; Zeng, D.; Xie, C. Comparative study on the visible light driven photocatalytic activity between substitutional nitrogen doped and interstitial nitrogen doped TiO2. *Applied Catalysis A: General* **2014**, *488*, 239–247.